Journal of Scientific and Technical Research
www.intellectink.in/ journal-of-scientific-and-technical-research
https://doi.org/10.67103/jstr/2026.16.1.11

Comparative Analysis of 2-Level and 3-Level Converter-Based Solar-MPPT DC Fast EV Charger

Ankita Singh[1], Pratima Walde[2], Manisha Rajoriya[3] and Suman Lata[4*]
[1,2,3,4]Department of Electrical Electronics and Communication Engineering,
Sharda School of Engineering and Science, Sharda University, Greater Noida,
Uttar Pradesh, India

Abstract:

The widespread adoption of electric vehicles (EVs) requires a power quality-compliant fast charging infrastructure. This paper presents a comparative performance analysis of a grid-integrated photovoltaic (PV) assisted DC fast EV charging station using maximum power point tracking (MPPT). The proposed system integrates a PV array, MPPT controller, grid interface, inverter, front-end converter, DC link regulation, and EV battery charging unit. The effectiveness of a three-level inverter and three-level front-end converter (3LI-3LFEC) is compared with a conventional two-level inverter and front-end converter (2LI-2LFEC). Performance evaluation was carried out using DC bus voltage regulation, EV charging power, PV power contribution, battery voltage, charging current, state-of-charge (SOC) variation, and harmonic analysis. Simulation results show both configurations maintain a stable DC bus voltage near 800 V. The three-level configuration EV charging power achieves 2.386% increase, and charging voltage and current reach approximately 926.61V and 102.90 A, respectively. The SOC increases from 0.2000 to 0.201833, validating successful battery energy transfer during the simulation interval. In (3LI-3LFEC) total harmonic distortion (THD) in current is reduced by 4.753%, whereas voltage THD is negligible in both configurations. Overall, the 3LI-3LFEC-based solar-assisted EV charging system provides improved charging performance and enhanced power quality for high-power DC fast-charging applications.

Keywords: *DC fast charger, solar PV, MPPT, three-level inverter, front-end converter, harmonic analysis, THD, power quality, grid integration*.

I. INTRODUCTION

Electric vehicles (EVs) are becoming a central component of sustainable transportation because they reduce dependence on fossil-fuel-based mobility and support the low-carbon energy transition. However, the rapid deployment of high-power DC fast charging stations introduces technical challenges for distribution networks, particularly regarding peak power demand, voltage regulation, harmonic distortion, power quality, and coordinated energy management. Recent reviews on EV charging infrastructure emphasise that DC fast charging station design must consider not only charging speed and converter efficiency, but also grid impact, converter topology, energy management, renewable energy integration, and operational reliability [1],[2]. To reduce the stress on the utility grid, renewable energy-supported EV charging stations have attracted considerable research attention. Among renewable sources, solar photovoltaic (PV) generation is most suitable for EV charging infrastructure because it can be locally installed, modularly expanded, and interfaced with charging stations through power electronic converters. PV assisted charging stations can reduce grid dependency, improve renewable energy utilization, and support cleaner charging operations. The intermittent nature of solar power requires proper maximum power point tracking (MPPT), grid support, and coordinated converter control to maintain reliable charging performance. Recent studies on PV-integrated renewable energy-based EV charging stations highlight the importance of power converter selection, MPPT control, grid interaction, and energy management strategies for stable and efficient operation. A DC fast charging station generally consists of multiple power conversion stages, including an AC to DC front-end converter, a regulated DC link, an isolated DC to DC converter, and an EV battery charging controller. In grid-connected operation, the frontend converter regulates the DC link voltage and controls the power drawn from the AC side, while the isolated DC to DC converter provides controlled charging current to the EV battery [3]. In simulation based fast charger studies, an 800 V DC link is commonly used for high power EV charging architectures, and the AC side filter and measurement blocks are important for observing line current, supply voltage, and harmonic behaviour. The MATLAB/Simscape DC fast charger reference model also represents the front-end converter as a unity power factor converter used to regulate the DC output at 800 V, with filtering and AC measurement blocks used for harmonic observation [4]. In the proposed work, a grid connected solar PV assisted DC fast EV charging system is developed in MATLAB/Simulink. The system integrates a solar PV array, MPPT controller, three level inverter, AC filter, utility grid, three level front end converter, isolated DC to DC converter, and EV battery pack. The PV plant is designed using data sheet-based module parameters with series connected modules and parallel strings to obtain an approximate rating of 35.12 kW. The PV voltage and current are processed by the MPPT controller to extract maximum available solar power, and the PV output is injected into the common three phase AC bus through a three-level inverter and AC filter. A 415 V, 50 Hz three phase grid is connected at the same AC bus to supply the remaining charging demand when solar generation is insufficient . Similar MATLAB/Simulink PV examples support datasheet-based PV plant sizing, MPPT techniques, and two level or three level inverter options for grid connected PV systems [5]. The use of multilevel converter topology is important in high power EV charging applications because converter switching behaviour directly affects voltage ripple, filter requirement, current distortion, and grid side power quality. Therefore, this work compares two level and three level converter-based charging configurations under similar operating conditions to evaluate their influence on EV charging power, DC link stability, battery charging current, PV contribution, requirement, grid power, efficiency, and harmonic distortion. Recent power quality studies on EV charging stations show that harmonic mitigation, load management, renewable coordination, and voltage stability analysis are essential for hybrid EV charging infrastructure [6],[25]. Harmonic assessment must be carefully performed at relevant measurement points, such as the PV inverter output, filter output, front end converter input, AC bus, DC link, and battery side. In addition, IEEE 519-2022 evaluates voltage distortion at the point of common coupling and uses current distortion limits based on the short circuit ratio, indicating that THD analysis should be interpreted with respect to the actual grid connection point and system rating [7]. The main contribution of this work is the development and comparative analysis of a MATLAB/Simulink based solar-assisted DC fast EV charging station with power quality focused evaluation. The proposed model includes a PV array with MPPT control, a grid-connected three-level-inverter, an AC filter, a 415 V three phase utility grid, a three level front end converter, an 800 V regulated DC link, an isolated DC to DC converter, and an EV battery pack initialised at 0.2 SOC with 50 Ah capacity. The EV charging current is regulated near 100 A, and voltage and current signals are measured at the solar side, filter side, front end converter input, DC link, and battery terminals [8]. The exported simulation data are used to calculate PV power, grid power, EV charging power, PV share, efficiency, SOC rise, DC link stability, FFT response, and THD before and after filtering. The study provides a detailed performance and harmonic comparison of two level and three level converter topologies for a renewable integrated, grid responsive, and power quality aware DC fast EV charging infrastructure[9],[10]. The paper has been organised as follows: Section 2 presents the detailed design of the proposed model in the methodology section. Section 3 presents the results and discussions, and Section 4 is focused on conclusions[19].

II METHODOLOGY

This section presents the design of the proposed model and a detailed description of all the simulation parameters. The details of the performance evaluation indicators are also presented.

A. Design of Proposed Model

The complete measurement, control and result extraction procedure of the proposed charger is shown in Fig. 1.

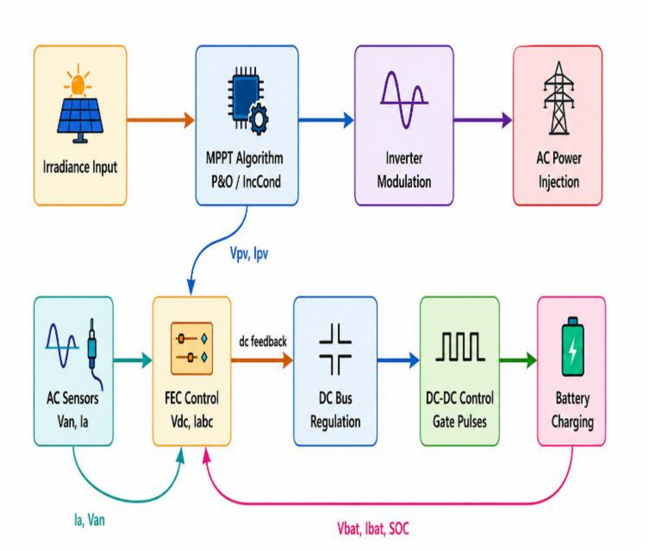

Fig.1 Control, Measurement, and Result Extraction Flow for the Solar-Assisted EV Charger

The model consists of a solar PV array, MPPT controller, three-level inverter, AC filter, utility grid, three-level front-end converter, isolated DC-DC converter, and EV battery pack, as shown in Fig. 2.

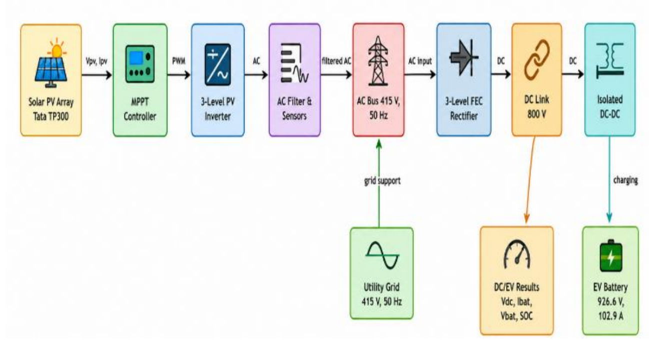

Fig.2 Solar MPPT Assisted DC Fast EV Charging Station using 3 Level Inverter and 3 Level FEC

The solar PV array was designed using datasheet-based parameters, with 39 modules connected in series per string and 4 parallel strings, giving an approximate PV rating of 35.12 kW. The PV voltage and current are given to the MPPT controller to extract the maximum available solar power[11]. The extracted PV power was then supplied to the three-phase AC bus through a three-level inverter and an AC filter. A 415 V, 50 Hz, three-phase utility grid was connected at the common AC bus to supply the remaining charging demand when PV power was insufficient[12],[13]. The DC fast charger used a three-level front-end converter (FEC) to regulate the DC link voltage at approximately 800 V. An isolated DC to DC converter was used to control the EV battery charging current at 100 A. The EV battery was initialized at 0.2 SOC with a rated capacity of 50 Ah. A grid connected solar PV assisted DC fast EV charging system was developed in MATLAB/Simulink. Voltage and current signals were measured at the solar side, filter side, FEC input side, DC link side, and battery side.

B. Model Description along with Simulation Parameters

The methodology is divided into PV source modelling, MPPT-based power extraction, AC grid integration, DC fast charging control, battery charging analysis, and post-processing of results [14],[27]. The same modelling structure is used for both two-level and three-level converter comparisons; only the converter topology selection is changed while the main PV, battery, and grid parameters are kept consistent [15],[16].

1) PV source and MPPT modelling

The solar cell selected for designing the PV system is the Tata Power Solar TP300 module. The main specifications of the selected solar cell are presented in Table 1 below.

Table 1. Solar cell equivalent-circuit parameters used for the PV array model

S.No	Solar Cell Parameter	Symbol	Value
1	Diode saturation current	Is	1.08146e-6 A
2	Second diode saturation current	Is2	5.42603e-9 A
3	Solar-generated current for measuring irradiance	Ir	8.71 A
4	Irradiance used for measurement	Ir0	1000W/m^2
5	Quality factor	N	1.523
6	Second diode quality factor	N2	1.871
7	Series resistance	Rs	0.000339 ohm
8	Parallel resistance	Rp	655.536 ohm
9	Solar Cell Parameter	Symbol	Value

The PV plant is modelled using a solar panel equivalent circuit. The plant consists of series connected modules per string and multiple parallel strings to achieve the desired PV power rating. The MPPT block receives PV voltage and current and adjusts the operating point so that the solar plant operates close to the maximum power point . In the present paper, perturb-and observe and incremental conductance MPPT options are available[24],[26]. The selected MPPT method has been kept identical so that the comparison reflects the converter topology effect rather than MPPT tuning differences. The intermediate DC to DC converter on the PV side has not been used. Table 2 presents the important parameters of the grid connected solar PV model [29],[30],[31].

Table 2. Grid-connected solar PV system parameters

S.No	Parameter	Symbol/Variable	Value
1	User-input PV power rating	P PV, rated	35.00Kw
2	Minimum panels per string	Ns, min	33 panels
3	Maximum panels per string before voltage limit	Ns, max	41 panels
4	Actual panels per string	Ns	39 panels
5	Parallel strings	Np	4 strings
6	Total panels	Ns x Np	156 panels
7	Actual PV plant power	P PV, actual	35.12kW
8	Minimum boost-less PV plant power	P PV, min	7.43kW
10	Maximum power possible per string	P string, max	9.23kW
11	MPPT options	MPPT	Incremental Conductance
12	Grid operating objective	UPF	Unity power factor

2) Grid-connected inverter and AC measurement stage

The PV inverter is connected to the three-phase AC bus through an AC filter and measurement block[17],[20]. In the proposed case, the three level inverter option is selected to reduce switching related distortion and improve power quality. The simulated 3 level inverter is given in Fig. 3 below.

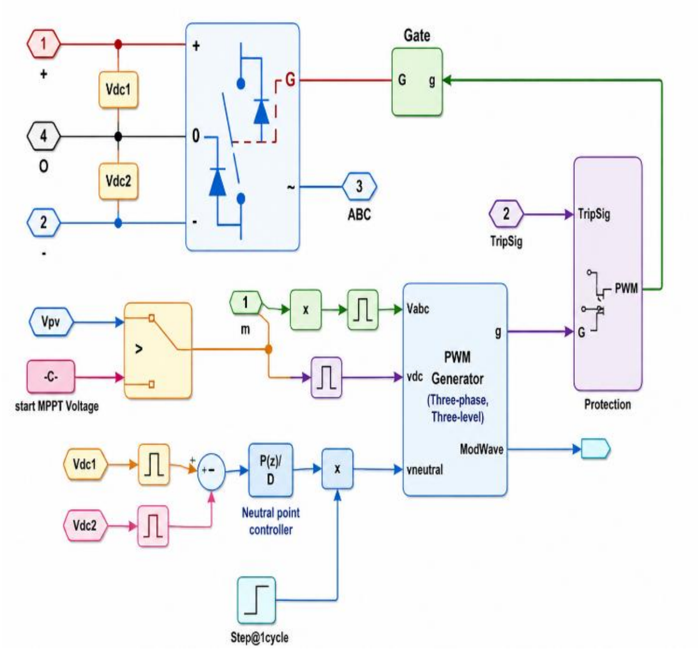

Fig.3 Three Level Inverter Power Circuit of Solar

Table 3. Front-end converter and rectifier parameters

Parameter	Value
Line-to-line RMS AC voltage	415 V
Phase-to-neutral RMS AC voltage	239.60 V
Peak phase voltage	338.85 V
DC-link voltage	800 V
Nominal DC current	700 A
System frequency	50 Hz
Switching frequency	10,000 Hz
Calculated AC current	1101.78 A
Maximum filter inductance	0.000168 H

3) DC fast charger and three-level FEC

The DC fast charging station receives three-phase AC power from the common AC bus. The front end converter regulates the DC bus at approximately 800 V. For the proposed topology, the FEC is configured as a three level converter [31],[28]. The three-level FEC provides lower current distortion and smoother DC link regulation than the two-level converter. The regulated DC link supplies an isolated DC to DC converter that controls the EV battery charging current[21],[22],[24].

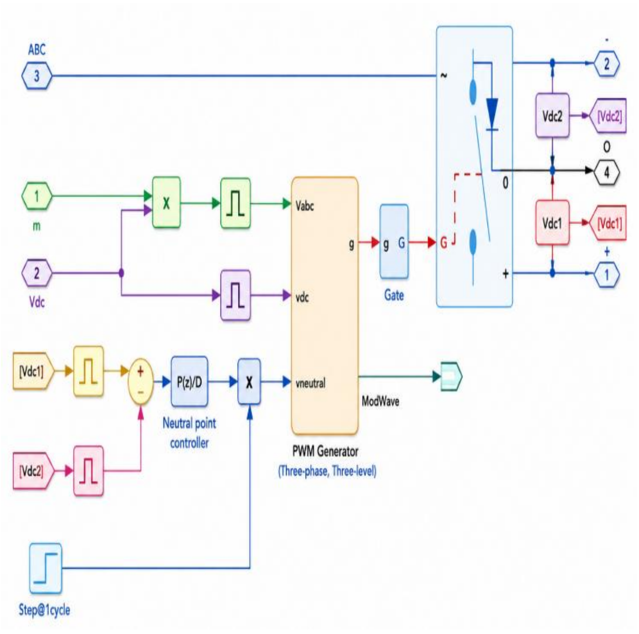

Fig.4 FEC 3 Level DC Fast charging

Table 4 gives the FEC control, sensing, and line parameters derived from the DC fast charger

Table 4. FEC line, sensing, and controller parameters

Parameter	Value
Line inductance	0.0001H
Line resistance	0.020 Ω
Line time constant	0.0050s
DC-link output capacitance	0.020F
Voltage sensor time constant	0.000010s
Current sensor time constant	0.000010s
Converter gain	400.0
Voltage ratio coefficient	0.423558
Total control delay	0.000130s
Current controller gain	0.002083
Voltage controller gain	181.612

4) Battery Charging

The EV battery pack is represented with an initial SOC of 0.2 and a rated capacity of 50 Ah. During simulation, charging voltage, charging current, and SOC are monitored. EV charging power is calculated from the battery terminal voltage and current. PV share, grid contribution, efficiency, and harmonic performance are then evaluated from the exported workspace data[18],[23].
Table 5 summarizes the DC to DC converter, transformer, chopper sensing and EV battery parameters used in the charging stage

Table 5. Choice of DC-DC converter, transformer, chopper sensing, and battery parameters

Stage	Parameter	Value
DC-DC converter	Switching frequency	10,000Hz
	PI controller gains	2, 1
	Inductance	10e-6H
Transformer	Magnetizing inductance	1H
	Winding factor	0.5
Chopper sensing	Voltage/current sensor gains	1, 1
	Voltage/current sensor time constants	10e-6s
Battery	Charging current reference	100A
	Initial SOC	0.2pu
	Capacity	50Ah
	Battery inductance	5e-3H
	Cell configuration	100, 1

Table 6 gives the simulation time and converter variant selection used for the two-level and three-level comparison

Table 6. Simulation time and converter variant selection

Parameter	Variable / Condition	Value
Number of simulated cycles	Simulation Number of Cycles	10
Simulation time	Simulation sim Time	0.2 s
Average FEC/inverter variant	Power Circuit 0	Average
Two-level variant	Power Circuit 1	Two-level
Three-level variant	Power Circuit 2	Three-level
Proposed final topology	Power Circuit	2

C. Performance Indicators for Evaluation

The following parameters have been considered for the performance evaluation of the proposed system.

I. PV output power: The solar PV output power is calculated as

$$P_{\mathrm{PV}} = \frac{V_{\mathrm{PV}} I_{\mathrm{PV}}}{1000} \qquad (1)$$

where $P_{\mathrm{PV}}$is the photovoltaic power in kW, V_{PV} is the PV voltage in volts, and I_{PV} is the PV current in amperes.

II. EV battery charging power: It is expressed as

$$P_{\mathrm{EV}} = \frac{V_{\mathrm{bat}} I_{\mathrm{bat}}}{1000} \qquad (2)$$

where $V_{\text{bat}}$and I_{bat} are the EV battery charging voltage and current, respectively.

III. DC-link power: It is obtained as

$$P_{\text{DC}} = \frac{V_{\text{DC}} I_{\text{DC}}}{1000} \qquad (3)$$

where $V_{\text{DC}}$is the DC-link voltage and $I_{\text{DC}}$is the DC-link current.

IV. PV power contribution : It is also known as PV share and is calculated as

$$\text{PV Share} = \frac{P_{\text{PV}}}{P_{\text{PV}} + P_{\text{grid}}} \times 100 \qquad (4)$$

V. Estimated grid contribution: It is the difference between the total input power supplied to the EV charging system (P_{input}) and the PV power contribution

$$P_{\text{grid}} = P_{\text{input}} - P_{\text{PV}} \qquad (5)$$

VI. Charging efficiency: The charging efficiency is calculated as

$$\eta = \frac{P_{\text{EV}}}{P_{\text{PV}} + P_{\text{grid}}} \times 100 \qquad (6)$$

VII. The rise in battery state of charge is determined by

$$\Delta SOC = SOC_{\text{final}} - SOC_{\text{initial}} \qquad (7)$$

VIII. Total harmonic distortion: The total harmonic distortion is calculated as

$$THD = \frac{\sqrt{X_2^2 + X_3^2 + X_4^2 + \cdots + X_n^2}}{X_1} \times 100 \qquad (8)$$

where X_1 is the fundamental component and $X_2, X_3, \ldots, X_n$are the harmonic components

The complete workflow is presented below in Fig.5

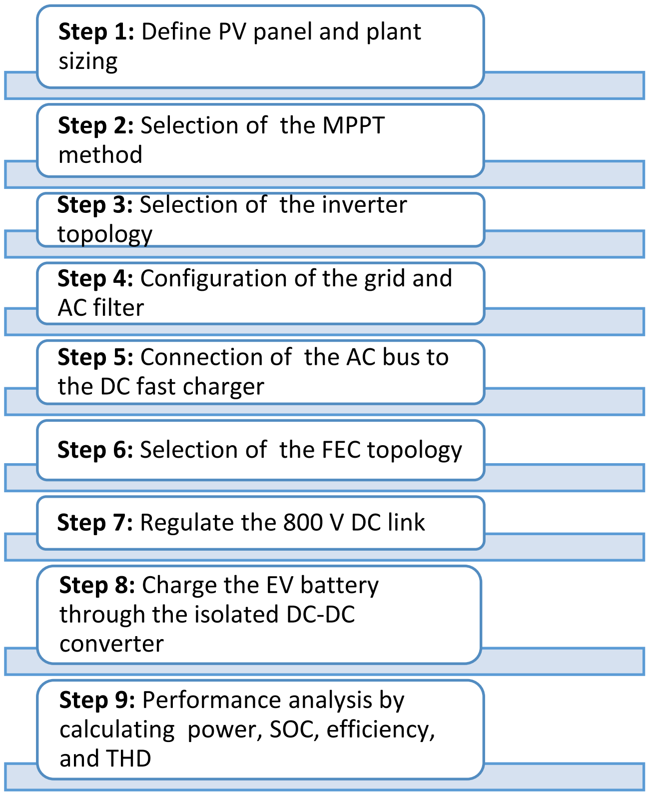

Fig.5 Flow chart of Methodology

III RESULTS AND DISCUSSIONS

This section summarizes the comparative simulation results for the solar MPPT assisted DC fast EV charging system using two converter configurations: **C1: 2 level inverter plus 2 level front end converter (FEC) and C2: 3 level inverter plus 3 level FEC**. The comparison includes DC bus regulation, EV charging power, grid contribution, PV contribution, harmonic performance, and SOC rise. The comparison of the two configurations, C1 and C2, in terms of harmonic distortion is shown in Table 7. The graphical representation is shown in Fig. 6. It can be concluded that the current THD is reduced from 4.755% to 4.529% in C2. Therefore, the 3 level configuration achieves a 4.753% reduction in current THD. Both configurations remain within the 5% current THD limit, but the 3-level converter provides better harmonic performance. The voltage THD remains almost negligible in both cases.

Table 7. Separate Harmonic Performance Comparison at Solar, Filter, and FEC Measurement Points

Measurement Point / Harmonic Parameter	C1	C2	Observation
Solar-side current THD (Ia)	4.755%	4.529%	3-Level gives lower THD
Filter-side current THD (Ia)	4.755%	4.529%	3-Level gives lower THD
FEC/EV input current THD (Ia)	4.755%	4.529%	3-Level gives lower THD
Voltage THD	0.000009 %	0.000019%	Both are very low
Acceptable current THD limit	5%	5%	Both are within the limit

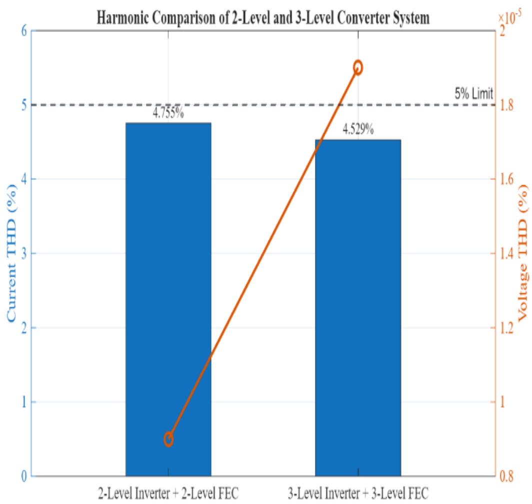

Fig.6 Harmonic Comparison of 2 Level and 3 Level EV Converter System

The comparative study of EV charging and battery performance in both configurations C1 and C2 is presented in Table 8.

Table 8. EV Charging and Battery Performance Comparison

Battery/EV Parameter	2-Level System	3-Level System	Result
DC bus voltage	800.000 V	799.998 V	Both regulate near 800 V
EV charging power	93.122 kW	95.344 kW	3-Level improves charging power
SOC rise	0.1833 percentage points	0.1833 percentage points	Both confirm charging
Battery charging condition	Charging	Charging	Valid for both
DC fast charging range	90 kW	90 Kw	Both valid DC fast charging systems

From Table 8, it is clear that the EV charging power in C1 is 93.122 kW and in C2 is 95.344 kW, indicating better performance of C2. The comparison of renewable power contribution in C1 and C2 is shown in Table 8.

Table 9. Renewable and Grid Power Contribution Comparison

Power Contribution	2-Level System	3-Level System	Observation
PV power	30.140 Kw	23.770 Kw	2-Level has higher PV contribution in this run
Grid contribution	65.514 kW	70.385 kW	3-Level uses slightly more grid power
PV share	31.509%	25.246%	2-Level has a higher PV share
EV charging power	93.122 kW	95.344 kW	3-Level delivers higher EV charging power

The 2-level system has higher PV power and PV share in this simulation case, with a PV contribution of 30.140 kW and PV share of 31.509%. The 3-level system has 23.770 kW PV power and 25.246% PV share. The 3-level system performs better in terms of EV charging power.

Table 10 compares the overall performance of the 2-level and 3-level converter-based solar-assisted EV charging systems.

Table 10. Overall Performance Comparison of C1 and C2 -Based EV Charging System

S.No	Performance Parameter	C1	C2	Better Configuration
1	DC bus voltage	800.000 V	799.998 V	Both stable
2	EV charging power	93.122 kW	95.344 kW	3-Level
3	PV power	30.140 kW	23.770 kW	2-Level in this run
4	Grid contribution	65.514 kW	70.385 kW	2-Level has lower grid use
5	PV share	31.509%	25.246%	2-Level in this run
6	Current THD	4.755%	4.529%	3-Level
7	Voltage THD	0.000009 %	0.000019 %	Both negligible
8	SOC rise	0.1833 percentage points	0.1833 percentage points	Both same

Both configurations maintain a stable DC bus voltage close to 800 V, confirming proper DC link regulation. In C2, EV charging power increases from 93.122 kW to 95.344 kW, corresponding to an improvement of 2.386% in comparison with C1. This confirms that the 3-level topology provides better charging power. Graphical presentation of EV charging power, PV power and grid power in C1 and C2 is presented in Fig.7.

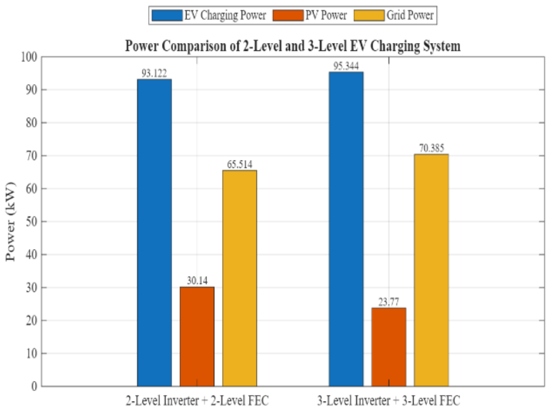

Fig.7 Power Comparison of 2 Level and 3 Level EV Charging Systems

IV Conclusions

The paper presented detailed simulation results for the solar MPPT assisted DC fast EV charging system using two converter configurations: 2 level inverter plus 2 level front end converter (C1) and 3 level inverter plus 3 level front end converter(C2). The C2 shows improvement in EV charging power and Current THD reduction parameters. The EV charging power shows 2.386% improvement in the C2 configuration. Additionally, there is 4.753% improvement in the current THD reduction. The battery charging voltage and current reach approximately 926.61 V and 102.90 A, respectively, confirming DC fast charging operation. The SOC shows a slight change from 0.2000 to 0.201833, validating successful battery energy transfer during the simulation interval. Voltage THD in both configurations are approximately the same, with a difference of 0.002 V. Both configurations can maintain the DC bus voltage at the same level, around 800 V.

V. Future Scope

In future, the proposed solar PV-assisted grid-connected DC fast EV charging station can be extended by integrating wind energy with solar PV and grid support to develop a hybrid renewable energy-based fast charging system. The addition of wind power can improve renewable power availability, reduce grid dependency, and enhance charging reliability under variable environmental conditions. Further improvement can be achieved by using advanced multilevel inverter topologies such as five-level, seven-level, cascaded H-bridge, neutral point clamped, flying capacitor, or modular multilevel converters, which can reduce switching stress, improve output voltage quality, minimize harmonic distortion, and increase overall efficiency. The MPPT controller can also be upgraded using advanced techniques such as fuzzy logic, artificial neural network, particle swarm optimization, genetic algorithm, sliding mode MPPT, or hybrid AI based MPPT to improve tracking speed and accuracy under rapid irradiance changes and partial shading conditions. In addition, future work may include battery energy storage, smart energy management, bidirectional V2G/G2V operation, and real time hardware in the loop validation to make the charging station more efficient, reliable, intelligent, and suitable for large scale EV charging infrastructure

REFERENCES

[1] Z. Ullah, L. Yan, A. U. Rehman, H. S. Qazi, W. Xiaodong, L. Jingkuan, and H. M. Hasanien, “Distributed consensus-based optimal power sharing between grid and EV charging stations using derivative-free charging scheduling,” IEEE Access, vol. 12, 2024.

[2] P. Shukl and B. Singh, “Distributed energy resources based EV charging station with seamless connection to grid,” IEEE Transactions on Industry Applications, vol. 59, no. 3, 2023.

[3] D. Ji, M. Lv, J. Yang, and W. Yi, “Optimizing the locations and sizes of solar assisted electric vehicle charging stations in an urban area,” IEEE Access, vol. 8, 2020.

[4] V. Jain, S. Kewat, and B. Singh, “Three phase grid connected PV based EV charging station with capability of compensation of reactive power,” IEEE Transactions on Industry Applications, vol. 59, no. 1, 2023.

[5] A. Verma and B. Singh, “Multimode operation of solar PV array, grid, battery and diesel generator set based EV charging station,” IEEE Transactions on Industry Applications, vol. 56, no. 5, 2020.

[6] S. Singh, P. Chauhan, and N. J. Singh, “Feasibility of grid-connected solar-wind hybrid system with electric vehicle charging station,” Journal of Modern Power Systems and Clean Energy, vol. 9, no. 2, 2021.

[7] G. H. Reddy, S. R. Depuru, S. Gope, B. V. Narayana, and M. N. Bhukya, “Simultaneous placement of multiple rooftop solar PV integrated electric vehicle charging stations for reliability benefits,” IEEE Access, vol. 11, 2023.

[8] B. Singh, A. Verma, A. Chandra, and K. Al-Haddad, “Implementation of solar PV-battery and diesel generator based electric vehicle charging station,” IEEE Transactions on Industry Applications, vol. 56, no. 4, 2020.

[9] S. Bagherwal and S. Mahapatra, “Enhanced stability and control of solar powered EV charging stations using disturbance observer-based adaptive sliding mode control for DC voltage stabilization,” IEEE Access, vol. 12, 2024.

[10] V. Jain, B. Singh, and Seema, “A grid connected PV array and battery energy storage interfaced EV charging station,” IEEE Transactions on Transportation Electrification, vol. 9, no. 3, 2023.

[11] N. A. El-Taweel, H. Farag, M. F. Shaaban, and M. E. AlSharidah, “Optimization model for EV charging stations with PV farm transactive energy,” IEEE Transactions on Industrial Informatics, vol. 18, no. 7, 2022.

[12] A. Verma and B. Singh, “AFF-SOGI-DRC control of renewable energy-based grid interactive charging station for EV with power quality improvement,” IEEE Transactions on Industry Applications, vol. 57, no. 1, 2021.

[13] A. K. Aktar, A. Taşcıkaraoğlu, O. Erdinç, and S. Güner, “Impacts of distribution-level joint scheduling of electric vehicle battery charging and swapping stations on reliability improvement,” IEEE Transactions on Industry Applications, vol. 60, no. 5, 2024.

[14] R. Zahedi, R. L. Sheinberg, S. N. Gowda, J. R. Chadha, K. SedghiSigarchi, and R. Gadh, “Phased planning of heavy-duty electric vehicle charging stations: An optimization framework under grid capacity constraints,” IEEE Access, vol. 14, 2026.

[15] M. M. Mahfouz and M. R. Iravani, “Grid-integration of battery-enabled DC fast charging station for electric vehicles,” IEEE Transactions on Energy Conversion, vol. 35, no. 1, 2020.

[16] S. Palanisamy and H. Lala, “Optimal sizing of renewable energy powered hydrogen and electric vehicle charging station (HEVCS),” IEEE Access, vol. 12, 2024.

[17] S. Rivera, S. M. Goetz, S. Kouro, P. W. Lehn, M. Pathmanathan, P. Bauer, and R. A. Mastromauro, “Charging infrastructure and grid integration for electromobility,” Proceedings of the IEEE, vol. 111, no. 4, 2023.

[18] V. Dhanawat, V. Shinde, R. Alami, A. Akhunzada, Z. B. Faheem, and A. Biswas, “Electric vehicles charging station load forecasting integration with renewable energy using novel Deep EfficientBiLSTMNet,” IEEE Open Journal of Vehicular Technology, vol. 6, 2025.

[19] Y. Jiang, T. Ortmeyer, and M. Fan, “Data-driven fast uncertainty assessment of distribution systems with correlated EV charging demand and renewable generation,” IEEE Transactions on Sustainable Energy, vol. 14, no. 3, 2023.

[20] M. Shalaby, “Planning smart EV charging infrastructure around metro transit hubs in Riyadh,” IEEE Access, vol. 13, 2025.

[21] H. Arya and M. Das, “Fast charging station for electric vehicles based on DC microgrid,” IEEE Journal of Emerging and Selected Topics in Industrial Electronics, vol. 4, no. 4, 2023.

[22] S. Barsali, R. Bojoi, M. Ceraolo, V. Mallemaci, F. Mandrile, S. Mocci, and G. Pasini, “Grid forming inverters for electric vehicle charging stations to enhance distribution grid resilience,” IEEE Access, vol. 13, 2025.

[23] M. M. Mahfouz and R. Iravani, “A supervisory control for resilient operation of the battery-enabled DC fast charging station and the grid,” IEEE Transactions on Power Delivery, vol. 36, no. 4, 2021.

[24] K. S. R. Sekhar, M. A. Chaudhari, and V. Khadkikar, “Enhanced hybrid converter topology for PV-grid-EV integration,” IEEE Transactions on Energy Conversion, vol. 38, no. 4, 2023.

[25] B. K. Saw and A. K. Bohre, “Sustainable deployment of EV charging stations in distribution network supported with hybrid solar-DG integrated DSTACOM,” IEEE Transactions on Industry Applications, vol. 61, no. 5, 2025.

[26] J. S. Tamba II, A. Abdulkarim, and A. N. Shuaibu, “Solar powered electric vehicle charging system: A comprehensive review,” Discover Electronics, vol. 2, Art. no. 96, 2025, doi: 10.1007/s44291-025-00139-x.

[27] A. R. Bhatti, M. Tamoor, R. Liaqat, A. Rasool, Z. Salam, A. Ali, and A. Sherefa, “Electric vehicle charging stations and the employed energy management schemes: A classification-based comparative survey,” *Discover Applied Sciences*, vol. 6, Art. no. 503, 2024, doi: 10.1007/s42452-024-06190-9.

[28] A. Karmakar, P. K. Sadhu, S. Das, S. P. Bihari, B. Khan, and A. Ali, "Techno-economic analysis and optimized PV-powered EV charging facilities under various climate conditions in India," *Discover Sustainability*, vol. 6, Art. no. 285, 2025, doi: 10.1007/s43621-025-01119-7.

[29] D. Mazumdar, H. A. Shuaibu, C. Sain, and T. S. Ustun, "A novel and sturdy MPPT architecture for grid-tied EV charging stations using Ali Baba and forty thieves optimization," *Discover Sustainability*, vol. 6, Art. no. 530, 2025, doi: 10.1007/s43621-025-01089-w.

[30] E. P. Sangeetha, N. Subashini, S. A. Lindiya, *et al*., "A distinctive optimized sliding mode control approach for grid-connected bidirectional DC-DC converters in DC fast charging stations with G2V and V2G support," *Electrical Engineering*, vol. 108, Art. no. 262, 2026, doi: 10.1007/s00202-026-03609-x.

[31] M. M. A. Ashiq, L. J. S. Shanthi, G. Sivasankar, *et al*., "Artificial neural network controlled canonical switching converter for electric vehicle charging applications," *Neural Computing and Applications*, vol. 38, Art. no. 306, 2026, doi: 10.1007/s00521-026-12009-y..